A major purpose of the Technical Information Center is to provide the broadest dissemination possible of information contained in DOE's Research and Development Reports to business, industry, the academic community, and federal, state and local governments.

Although a small portion of this report is not reproducible, it is being made available to expedite the availability of information on the research discussed herein.

LA-UR -87-140

LA-UR--87-140

DE87 005106

TITLE NONLINEAR RESPONSE MATRIX METHODS FOR RADIATIVE TRANSFER

AUTHOR(S) Warren F. Miller, DDERT

Elmer E. Lewis, Consultant (Northwestern University)

SUBMITTED TO International Topical Meeting on Advances in Reactor Physics, Mathematics and Computation, Meridien Montparnasse Hotel, Paris, France, April 27-30, 1987

DISCLAIMER

Los Alamos Los Alamos National Laboratory
Los Alamos, New Mexico 87545

NONLINEAR RESPONSE MATRIX METHODS FOR RADIATIVE TRANSFER*

W. F. Miller, Jr
Los Alamos National Laboratory
Los Alamos, New Mexico 87545
(505) 667-7978

and

E. E. Lewis+
Northwestern University
Evanston, Illinois 60201
(312) 491-3579

ABSTRACT

A nonlinear response matrix formalism is presented for the solution of time-dependent radiative transfer problems. The essential feature of the method is that within each computational cell the temperature is calculated in response to the incoming photons from all frequency groups. Thus the updating of the temperature distribution is placed within the iterative solution of the space-angle transport problem, instead of being placed outside of it. The method is formulated for both grey and multifrequency problems and applied in slab geometry. The method is compared to the more conventional source iteration technique.

I. INTRODUCTION

The response matrix method has enjoyed considerable success in the neutron transport community for a reasonably wide class of problems[1,2]. Since the method involves an iteration on the particle flux at spatial cell boundaries, experience indicates that the approach is most efficient when spatial cells are optically thick. Then, the number of boundary crossings by particles is comparatively small. On the other hand, when there are many optically thin cells, particles cross many cells before being absorbed or leaking and many boundary crossings are involved to achieve a solution.

There is a class of nonlinear radiation transfer problems for which the response matrix approach seems promising. In these problems, the material satisfies the requirements of local thermodynamic equilibrium but the radiation and material energy densities are not generally in equilibrium.[3] This situation applies in many problems involving stellar or other high temperature, radiating media. When the radiating medium contains at least some moderately high Z material, the spatial cells can be very optically thick to photons.

There is another motivation for considering response matrix approaches for this class of radiation transfer problems. The basic idea of the nonlinear response matrix method developed in this paper is to solve for the local cell temperature as well as the outflow of radiation, assuming that only incoming photon intensity is known. The frequency spectrum of the reemitted radiation is a function of only the local cell temperature. Heuristically, by calculating a new temperature and emission spectrum as one sweeps the spatial mesh, the microscopic physics of the problem is more faithfully followed. Thus, in principle the process should converge rapidly.

*This work was performed under the auspices of the U.S. Department of Energy
+ Consultant, Los Alamos National Laboratory

In this paper we examine these arguments by applying response matrix methods to time-dependent radiation transfer problems and comparing the results with existing methods. In section II we formulate the response matrix in the grey approximation and compare it to two alternative algorithms for a series of model problems. In section III the method is generalized to a multifrequency formalism and applied to a 30 group-time-dependent problem in slab geometry.

II. GREY RADIATIVE TRANSFER

The transport of radiation in a physical medium depends inherently upon the frequency of the radiation. This is because the properties of the medium are frequency-dependent and because, when heated, the medium radiates photons of a wide range of frequencies. However, in order to clearly describe the response matrix approach and unambiguously compare its characteristics to other approaches, we first consider the grey case in which physical processes are independent of frequency. We further assume for simplicity that the specific heat and opacity are independent of the material temperature and are spatially constant.

A. The Basic Equations

The starting point for he calculations is the time-dependent grey thermal radiation transfer equation for the photon intensity, $I(\vec{r},\hat{\Omega},t)$,

$$\left[\frac{1}{c}\frac{\partial}{\partial t} + \hat{\Omega}\cdot\vec{\nabla} + \sigma\right]I(\vec{r},\hat{\Omega},t) = \sigma acT(\vec{r},t)^4. \qquad (1)$$

We also define the angularly integrated intensity

$$\phi(\vec{r},t) = \int d\Omega I(\vec{r},\hat{\Omega},t),$$

and $T(\vec{r},t)$ as the absolute material temperature, In Eq. (1), the notation is standard[4] with $\vec{r}$ denoting spatial location, Ω the direction of photon travel and t, the time. In Eq. (1), the temperature term describes the photon emission where a is the radiation constant, c is the speed of light, and σ is the macroscopic absorption coefficient or opacity depending upon the units used. Owing to the fact that the emission of photons by material is dependent upon the fourth power of the temperature, the equation is nonlinear in T.

We next require an energy conservation equation to provide an expression for the temperature. The energy equation is

$$c_v\frac{\partial}{\partial t}T(\vec{r},t) = \sigma\phi(\vec{r},t) - \sigma acT(\vec{r},t)^4 + W(\vec{r},t), \qquad (2)$$

where c_v is the specific heat and W is an external source of energy to the material. For many applications,[5] the constant specific heat assumption used here is a reasonable approximation. The assumption of a constant opacity is not as defensible but serves the purpose of allowing simple but meaningful test cases for comparing matrix solution algorithms.

The above equations imply assumptions about the physical problem other than those already described. Namely, we assume that the background material is stationary, thermal radiative emission is governed by local thermodynamic equilibrium in the matter, and scattering processes, thermal conduction and convection can be ignored. There are important classes of problems for which all these assumptions are reasonable.[3]

B. Time Differencing

In each of the approaches considered here we assume implicit time differencing of the equation of radiative transfer. Thus

$$[\hat{\Omega}\cdot\vec{\nabla} + \tilde{\sigma}]I(\vec{r},\hat{\Omega}) = \sigma acT(\vec{r})^4 + \tau I'(\vec{r},\hat{\Omega}), \tag{3}$$

where we define

$$\tau = \frac{1}{c\Delta t} \tag{4}$$

and

$$\tilde{\sigma} = \sigma + \tau$$

In Eq. (3), all quantities are defined at time t except I' and T', where the prime indicates evaluation at the preceding time step. (Note that if the opacity is temperature dependent it is assumed to be evaluated using the old temperature so in this case the method is not implicit in the strictest sense of the word.) Implicit differencing of the energy equation, Eq. (2), yields a transcendental relationship for the temperature in terms of the photon distribution

$$\sigma acT(\vec{r})^4 = \frac{\sigma\phi(\vec{r}) + c_v\tau T'(\vec{r}) + W(\vec{r})}{1 + \frac{c_v\tau}{\sigma' a} T(\vec{r})^{-3}} . \tag{5}$$

Several methods have been proposed for solving this set of equations. The first of these, which we call Method I, involves a straightforward iteration:

$$[\hat{\Omega}\cdot\vec{\nabla} + \tilde{\sigma}]I_{k+1/2}(\vec{r},\hat{\Omega}) = \sigma' acT_k(\vec{r})^4 + \tau I'(\vec{r},\hat{\Omega}), \tag{6}$$

$$\phi_{k+1/2}(\vec{r}) = \int d\Omega I_{k+1/2}(\vec{r},\hat{\Omega}), \tag{7}$$

and

$$\sigma' acT_{k+1}(\vec{r})^4 = \frac{\sigma\phi_{k+1/2}(\vec{r}) + c_v\tau cT'(\vec{r}) + W(\vec{r})}{1 + \frac{c_v\tau}{\sigma' a} T_{k+1}(\vec{r})^{-3}} , \tag{8}$$

where k is the iteration index. In this approach, a radiation transfer calculation Eq. (6) is performed assuming a known temperature, $T_k(\vec{r})$. This step is equivalent to a pure absorber solution in neutron transport. The result is then used in Eqs. (7) and (8) to calculate a new temperature. Note that one can consider several methods to accelerate the iteration,[5] but in order to allow consistent comparisons, we don't employ any acceleration approaches in the present work.

Method II is a slight variation of Method I, in which the iteration strategy is altered, but the relationship for the temperature is not modified. Namely, we insert Eq. (5) into Eq. (3), yielding the iteration equation

$$[\hat{\Omega}\cdot\vec{\nabla}+\tilde{\sigma}]I_{k+1}(\vec{r},\hat{\Omega}) = \frac{\sigma\phi_k(\vec{r})}{[1+\frac{c_v\tau}{\sigma' a} T'(\vec{r})^{-3}]} + \frac{c_v c\tau T'(\vec{r}) + W(\vec{r})}{[1+\frac{c_v\tau}{\sigma' a} T'(\vec{r})^{-3}]} + \tau I'(\vec{r},\hat{\Omega}) \tag{9}$$

and

$$\phi_{k+1}(\vec{r}) = \int d\Omega I_{k+1}(\vec{r},\hat{\Omega}), \tag{10}$$

where in Eq. (9), we have approximated T^{-3} with its value at the previous time step. Equations (9) and (10) constitute an iteration on the angularly integrated intensity that is analogous to a scattering iteration in neutronics.[6] Upon convergence, Eq. (5) is solved for the current temperature, again with T^{-3} evaluated at the previous time step. Method II was suggested by Fleck and Cummings, but with a slightly different approximation for the new temperature. This modified approach is not considered here since the alternative temperature expression should not affect the computational efficiency of the iteration.

C. Response Matrix Method

We next consider a response matrix, Method III, that in some respects is analogous to the response matrix methods appearing in the neutron transport literature.[1,2] We again use implicit differencing of the radiation transfer equation so our starting point is Eq. (3). We divide the spatial domain into volume elements V_i each with a surface L_i with outward normal n_i. In each volume element the temperature is assumed to have a value T_i that is uniform in space. Clearly, the number of volume elements selected must be large enough so that the assumption of constant temperatures is reasonable. In the numerical results to follow, the volume elements are identical to the spatial mesh on which the equations are differenced. Equation (3) becomes

$$(\hat{\Omega}\cdot\vec{\nabla} + \tilde{\sigma}_i)I(\vec{r},\hat{\Omega}) = \sigma_i acT_i^4 + \tau I'(\vec{r},\hat{\Omega}) \quad , \qquad \vec{r}\in V_i .$$

The solution of the transport equation in V_i may be written as a superposition of three solutions:

$$I(\vec{r},\hat{\Omega}) = I_u(\vec{r},\hat{\Omega}) + I_t(\vec{r},\hat{\Omega}) + I_e(\vec{r},\hat{\Omega})\, acT_i^4 , \qquad \vec{r}\in V_i .$$

These are taken to satisfy the following three equations:

$$[\hat{\Omega}\cdot\vec{\nabla} + \tilde{\sigma}_i]I_u(\vec{r},\hat{\Omega}) = 0 , \qquad \vec{r}\in V_i ,$$

$$I_u(\vec{r},\hat{\Omega}) = I(\vec{r},\hat{\Omega}) , \qquad \vec{r}\in \Gamma_i , \qquad \hat{\Omega}\cdot\hat{n}_i < 0 \tag{11}$$

$$[\hat{\Omega}\cdot\vec{\nabla} + \tilde{\sigma}_i]I_t(\vec{r},\hat{\Omega}) = \tau I'(\vec{r},\hat{\Omega}) , \qquad \vec{r}_i\in V_i , \tag{12}$$

$$I_t(\vec{r},\hat{\Omega}) = 0 , \qquad \vec{r}\in \Gamma_i , \qquad \hat{\Omega}\cdot\hat{n}_i < 0$$

and

$$[\hat{\Omega}\cdot\vec{\nabla} + \tilde{\sigma}_i]I_e(\vec{r},\hat{\Omega}) = \sigma_i , \qquad \vec{r}\in V_i \tag{13}$$

$$I_e(\vec{r},\hat{\Omega}) = 0 , \qquad \vec{r}\in \Gamma_i , \qquad \hat{\Omega}\cdot\hat{n}_i < 0$$

The first contribution I_u refers to the uncollided photons that have not yet been absorbed since crossing into V_i during the current time increment Δt. The second contribution, I_t, consists of those photons that have occupied V_i since the preceding time step, again without being absorbed. The last term is composed of the emitted photons.

Since I_u, I_t and I_e do not depend upon the current temperature in the volume element V_i, they can be calculated in terms of the photons entering the cell across L_i and those brought forward from the preceding time step, $t-\Delta t$. The corresponding angularly integrated quantities ϕ_u, ϕ_t, and ϕ_e, can be determined by integrating the angular intensities over all angles. Then denoting the cell volume average by $\bar{\phi}$, we may write

$$\bar{\phi} = \bar{\phi}_u + \bar{\phi}_t + \bar{\phi}_e acT_i^4. \tag{14}$$

To calculate the cell temperature, we combine this expression with Eq. (5), averaged over the cell. The result is a transcendental equation for the temperature in element V_i

$$\sigma_i acT_i^4 = \frac{[\sigma'(\bar{\phi}_u+\bar{\phi}_t) + c_v c_\tau T_i' + W]}{(1-\bar{\phi}_e + \frac{c_v \tau}{\sigma' a} T_i^{-3})}. \tag{15}$$

The response matrix equations require that Eqs. (11), (12), and (13) be discretized in the spatial and angular variables. We will describe a specifically selected differencing in the next section. The result from applying this differencing is a set of matrix equations for the average and exiting intensities for volume element i, given the incoming intensities:

$$\underline{I}^+ = \underline{R}\,\underline{I}^- + \underline{H}\,\underline{I}' + \underline{K} acT_i^4$$

and

$$\bar{I} = \tilde{\underline{R}}^T \underline{I}^- + \tilde{H}\,\bar{I}' + \tilde{K} acT_i^4.$$

In the equations, $\underline{I}^-$ refers to the incoming intensity; $\bar{I}$ refers to the element average intensity, and $\underline{I}^+$ refers to outgoing intensity. The $\underline{R}$, $\underline{H}$, and $\underline{K}$ are referred to as response matrices. The specific values of the matrices depend upon the angular and spatial difference schemes employed. In the response matrix approach the incoming intensities are assumed to be known for a given volume element and the above equations are solved for consistent outgoing intensities, average intensities and temperatures. One marches through the cells iterating on these cell edge intensities.

D. Space-Angle Discretization

To examine the computational efficiency of the solution strategies discussed above, slab geometry computer codes were developed that use discrete ordinates[6] to discretize the angular variable and the step characteristic method[7] to difference the equations in space. The codes were written to parallel one another as much as possible in order to facilitate timing comparisons. For the purpose of developing the difference equations, we write the equation of radiative transfer as

$$[\mu \frac{\partial}{\partial x} + \tilde{\sigma}] I(x,\mu) = \sigma_i S_i + \tau I'(x,\mu)$$

with

$$S_i = acT_i^4 \tag{16}$$

for Method I and the Response Matrix Method, and

$$S_i = \frac{[\bar{\Phi}_j + (c_v c\tau T_i' + W)/\sigma]}{[1 + \frac{c_v \tau}{\sigma' a}(T_i')^{-3}]} \tag{17}$$

for Method II. Within a spatial cell depicted in Fig. 1, and for a discrete ordinates direction denoted by m, we divide I_m into three contributions for each of the discrete directions.

$$I_m(x) = I_{um}(x) + I_{tm}(x) + I_{em}(x)S_i \qquad x_i - 1/2 \leq x \leq x_i + 1/2$$

Then Eqs. (11), (12), and (13), become

$$[\mu_n \frac{\partial}{\partial x} + \sigma_i] I_{um}(x) + \tau\bar{I}_{um} = 0 \quad , \qquad x_i - 1/2 \leq x \leq x_i + 1/2 \, ,$$

$$I_{um}(x) = I_m(x) \qquad x = x_{i-1/2} \, , \ \mu_m > 0 \, ,$$

$$x = x_{i+1/2} \, , \ \mu_m < 0 \, ,$$

$$[\mu_m \frac{\partial}{\partial x} + \sigma_i] I_{tm}(x) + \tau\bar{I}_{tm} = \tau\bar{I}_m' \qquad x_{i-1/2} \leq x \leq x_{i+1/2} \, ,$$

$$I_{tm}(x) = 0 \qquad x = x_{i-1/2} \, , \ \mu_m > 0 \, ,$$

and

$$x = x_{i+1/2} \, , \ \mu_m < 0 \, ,$$

$$[\mu_m \frac{\partial}{\partial x} + \sigma_i] I_{em}(x) + \tau\bar{I}_{em} = \sigma_i \, , \qquad x_{i-1/2} \leq x \leq x_{i+1/2} \, ,$$

$$I_{em}(x) = 0 \qquad x = x_{i-1/2} \, , \ \mu_m > 0 \, ,$$

$$x = x_{i+1/2} \, , \ \mu_m < 0 \, .$$

Note that we have replaced $\tau I(x)$ by $\tau\bar{I}$, the cell average value. This is done to insure that in the limit as $\Delta t \to \infty$, the correct steady state solution results.

Now approximating S by the cell average value, $\bar{S}$, and analytically solving the equation of transfer assuming a known incoming intensity, the step characteristic equations result

$$I_m(x_{i \pm 1/2}) = R_m I_m(x_{i \mp 1/2}) + H_m \bar{I}_m'(x_i) + K_m \bar{S}_i, \qquad \mu_m \gtrless 0 \tag{18}$$

and

$$\bar{I}_m(x_i) = \tilde{R}_m I_m(x_{i \mp 1/2}) + \tilde{H}_m \bar{I}_m'(x_i) + \tilde{K}_m \bar{S}_i \quad , \qquad \mu_m \gtrless 0. \tag{19}$$

The coefficients are given in Table 1 for $\Delta = x_{i+1/2} - x_{i-1/2}$. The angularly integrated intensity may be obtained from

$$\phi = \phi_u + \phi_t + \phi_e S$$

with

$$\phi_u = 1/2 \sum_{m=1}^{N/2} w_m \tilde{R}_m [I_{um}(x_{i+1/2}) + I_{um,N-m+1}(x_{i-1/2})] , \tag{20}$$

$$\phi_t = 1/2 \sum_{m=1}^{N/2} w_m \tilde{H}_m [\bar{I}_m'(x_i) + \bar{I}'_{N-m+1}(x_i)] \tag{21}$$

and

$$\phi_e = \sum_{m=1}^{N/2} w_m \tilde{B}_m . \tag{22}$$

E. Implementation

Equations (18) and (19) serve as the basis for all three iterative methods. In all cases, photons are tracked from left to right from spatial cell to spatial cell for each positive discrete ordinates direction and then from right to left for each negative direction. (We assume a set of directions that are symmetric about $\mu = 0$). The methods differ in the iteration strategy and therefore the treatment of the quasisources in Eqs. (18) and (19). In Method I the entire space-angle mesh is swept using Eq. (16) for the quasisource with the temperature for the previous iteration inserted. The angularly integrated intensities are calculated at each space point using Eqs. (20) through (22). Finally, the Newton-Raphson Method is used to solve Eq. (15) for an updated temperature to be used in Eq. (16) for the next iteration. In Method II, the mesh is swept using Eq. (17) for the quasisource. Iterations on the angularly integrated intensities continue until convergence. Then the temperature at the time step is calculated only once using Eq. (15) with T^{-3} used from the previous time step. Recall that Method II is not fully implicit since the temperature appearing in the denominator of Eq. (17) is evaluated at the previous time step. (Of course none of the methods are truly implicit if the opacity is temperature-dependent and evaluated at the previous time step.)

In Method III, the Response Matrix Method, the temperature is updated cell-by-cell as the sweeps progress. For a given direction and cell, Eq. (16) is used for the quasisource using the latest value of the temperature. Outgoing and average intensities are calculated using the latest values of the incoming intensities. Then Eqs. (20) through (22) are used to calculate angular integrated intensities for the cell. Next, the cell temperature is calculated from a Newton-Raphson solution of Eq. (15). With this new temperature, a new source is calculated from Eq. (16) and is used the next time the cell in question is solved. The calculation then proceeds to the next cell and direction.

To compare the iterative strategies in the grey approximation we have written three computer codes. The spatial differencing and other characteristics that are common to the methods are treated by identical algorithms to ensure the validity of timing comparisons. In the grey model problem an isotropic

intensity is applied at t=0 to the left boundary of a slab. There are no incoming photons on the right boundary. We consider several slab thicknesses, made up of N cells each of thickness Δ. The iteration is considered converged for each time step when the relative change in the reflection from the left boundary and the transmission through the slab are each less than 10^{-5}. The material parameters are taken to be $\sigma = 1.0\ cm^{-1}$, $C_v = 81.18\ ergs/(cm^3 \cdot KeV)$. All calculations are performed with an S_4 Gaussian quadrature set.[6]
The first set of calculations consisted of steady state solutions to assure that all three methods give identical results with $\tau = 0$. These calculations also verify that the spatial truncation error associated with step characteristic is second order. Table 2 indicates the computer run times and iteration counts for the steady state problem. Only two sets of results are presented since in the steady state limit of $\tau=0$, Methods I and II reduce to the same algorithm. In general, both the computing times and the numbers of iterations are smaller for the response matrix method than for the standard method, with the most dramatic improvements occuring - as expected - when the mesh spacing becomes coarse and/or the optical thickness of the slab becomes large. However, even for small mesh spacings and optically thin systems, where one would expect the response matrix technique to be at a disadvantage, the computing times are smaller than for the standard method.

For the time dependent problem, calculations are carried out both for temperature independent specific heat and for a problem in which the specific heat is artifically taken to be proportional to the cube of temperature in order to obtain linear equations. The reflection and transmission begin at zero and rise to asymptotic solutions of the steady state values obtained in the steady state problem. The accuracy of the transient solutions is found to be of first order in time. However, Method II cannot be used for the nonlinear case in which the specific heat is constant; the nonimplicit time differencing causes the iteration to diverge unless some physically artificial time step control procedure is employed.

For all methods, the number of iterations per time step decreases as time progresses, and the solution approaches the steady state values. This is to be expected since the rate of intensity change decreases with time. Once again the response matrix approach requires fewer iterations per time step than either of the other two methods. Even though the computer time per iteration is moderately longer for the response matrix method, the total computing time is always shorter with differences that are most dramatic for long time steps (i.e. small values of τ). This is illustrated in Table 3, where the computing times for the methods are compared. It should be noted that these results are for optically thin cells, and thus the response matrix algorithm may be expected to improve relative to the others when coarser meshes are used.

III. MULTIFREQUENCY RADIATIVE TRANSFER

The more realistic situation in radiative transfer allows the intensity to depend upon photon frequency. We consider the same problem description as in the grey case. Namely, the background matter is stationary, the thermal radiative emission is governed by local thermodynamic equilibrium, and scattering and thermal conduction can be neglected.

A. Basic Equations

To derive the response matrix method for the multifrequency case, we begin with the frequency-dependent radiative transfer equation for a volume element V_i:

$$\left[\frac{1}{c}\frac{\partial}{\partial t} + \hat{\Omega}\cdot\vec{\nabla} + \sigma(\nu,T_i)\right]I(\vec{r},\hat{\Omega},\nu,t) = \sigma(\nu,T_i)B(\nu,T_i) \quad , \quad \vec{r}\varepsilon V_i, \quad (23)$$

where ν is the photon frequency and $B(\nu,T_i)$ is the Planckian distribution at temperature T defined by

$$B(\nu,T) = \frac{2h\nu^3}{c^2}(e^{h\nu/kT}-1)^{-1}.$$

Associated with Eq. (23) is an energy balance equation

$$c_v\frac{\partial T_i}{\partial t} = \int d\nu\sigma(\nu,T_i)\phi_i(\nu,t) - a\sigma cT_i^4 + W_i, \quad (24)$$

where

$$\phi_i(\nu,t) = \frac{1}{V_i}\int_{V_i} dV\int d\Omega I(\vec{r},\hat{\Omega},\nu,t)$$

and

$$\sigma = \frac{\int d\nu B(\nu,T_i)\sigma(\nu,T_i)}{\int d\nu B(\nu,T_i)} \quad . \quad (25)$$

We again assume that the specific heat is independent of temperature. In implementing the response matrix formalism, we assume that the distribution of incoming photons in V_i is known. In turn, the energy deposition in V_i, the new temperature T_i, and the distribution of exiting photons can be calculated. The implementation again requires differencing the time, frequency, angular and spatial variables. In the following, we proceed in a matter analogous to the grey case and therefore abbreviate the development.

B. Time and Frequency Discretization

We apply implicit time differencing to Eq. (23) and (24) evaluating the opacity at the previous time step to obtain

$$[\hat{\Omega}\cdot\vec{\nabla} + \sigma(\nu) + \tau]I(\vec{r},\hat{\Omega},\nu) = \sigma(\nu)B(\nu,T_i) + \tau I'(\vec{r},\hat{\Omega},\nu) \quad , \quad \vec{r}\varepsilon V_i \quad (26)$$

and

$$c_v\tau cT_i = \int d\nu\sigma(\nu)\phi_i(\nu) - \sigma_i acT_i^4 + W + c\tau c_p T_i' \quad , \quad \vec{r}\varepsilon V_i. \quad (27)$$

We next define frequency groups $\nu_o < \nu_1 \cdots < \nu_{g-1} < \nu_g \cdots < \nu_G$, and define the frequency group intensity by

$$I_g(\vec{r},\hat{\Omega}) = \int_{\nu_g}^{\nu_{g-1}} d\nu I(\vec{r},\hat{\Omega},\nu)$$

Integrating Eqs. (26) and (27) over a frequency interval yields

$$(\hat{\Omega}\cdot\vec{\nabla} + \sigma_g' + \tau)\, I_g(\vec{r},\hat{\Omega}) = \sigma_g' B_g(T_i) + \tau I_g'(\vec{r},\hat{\Omega}) \quad , \quad \vec{r}\varepsilon V_i$$

and

$$c_v\tau cT_i = \sum_g \sigma_g'\bar{\phi}_{gi} - \bar{\sigma}_i' acT_i^4 + W + c_v\tau cT_i' \quad \vec{r}\varepsilon V_i, \quad (28)$$

where σ_g is the conventional multifrequency cross section,

$$B_g(T_i) = \int_{\nu_g}^{\nu_{g-1}} d\nu B(\nu,T_i)$$

and

$$\sigma_i = \frac{\sum_g \sigma_g(T_i)B_g(T_i)}{\sum_g B_g(T_i)} .$$

C. Response Matrix Formalism

We again divide the photon intensity into three contributions:

$$I_g(\vec{r},\hat{\Omega}) = I_{gu}(\vec{r},\hat{\Omega}) + I_{gt}(\vec{r},\hat{\Omega}) + I_{ge}(\vec{r},\hat{\Omega})B_g(T_i) , \qquad \vec{r}\varepsilon V_i . \quad (29)$$

If the group indexing is deleted then I_u, I_t and I_e satisfy Eqs. (11) (12) and (13).

As in the grey case, the sequence of calculations involves first determining I_{gu} and I_{gt} from Eqs. (13) and (14) given the latest incoming and average intensities. This calculation does not require knowledge of the cell temperature. Using the angularly integrated values of these intensities, a new temperature can be calculated from Eqs. (28) and (29). To derive a convenient expression for the temperature, we insert Eq. (29) into Eq. (28) to obtain

$$c_v\tau cT_i = \sum_g \sigma_g(T_i')(\bar{\phi}_{gu} + \bar{\phi}_{gt}) + \sum_g \sigma_g(T_i')\,\bar{\phi}_{ge}B_g(T_i) - \sigma(T_i)acT_i^4 + W_i + c\tau c_p T_i' . \quad (30)$$

From Eq. (25), we may write

$$1 = \frac{\sigma(T_i)\sum_g B_g(T_i)}{\sum_g \sigma_g(T_i)B_g(T_i)} = \frac{\sigma(T_i)acT_i^4}{\sum_g \sigma_g(T_i)B_g(T_i)} .$$

Using this expression in Eq. (30), we obtain

$$\sigma(T_i)ac\left[1 - \frac{\sum_g \sigma_g(T_i')B_g(T_i')\bar{\phi}_{gei}}{\sum_g \sigma_g(T_i')B_g(T_i')}\right] T_i^4 + c\tau c_v T_i = \sum_g \sigma_g(T_i')(\phi_{gu} + \phi_{gt}) + W_i + c_v\tau cT_i' . \quad (31)$$

Inside the brackets on the left side of Eq. (31), we have replaced T by T' to simplify the solution of the transcendental expression for T. If the opacity is not a strong function of temperature, no significant error should be introduced by this simplification.

D. Implementation

The implementation of the response matrix method requires that the foregoing multifrequency formulation be combined with space-angle differencing of the equations. Since this is carried out in a manner completely analogous to the grey case, it is not repeated here. We have written a multifrequency code for treating time-dependent radiative transfer problems in slab geometry using either step characteristic or diamond differencing on the spatial variable.

For multifrequency problems we have compared our results with those published for the temperature distributions of ref. (5), and the agreement is excellent. One problem considered consists of a 20 cm slab initially at 1 ev temperature and an analytic opacity given by $27(1-\exp(-\nu/KT))]/\nu^3$. At t = 0 a 1 Kev source is placed at the left. In Fig. 1 is shown the fractional energy deposition from the 20 cm slab as a function of time. The case for transmitted energy is particularly interesting, since it shows an increase at 2/3 nanoseconds, the time when the uncollided radiation first arrives at the right-hand face, and a second increase at about seven nanoseconds, when the material in the vicinity of the right boundary has heated sufficiently for significant amounts of emitted radiation to escape to the right. The transient timing comparisons, given in Table 1 for the temperature at 10 nanoseconds. In the steady state calculations the same problem is shown but with τ = 0; the diamond differencing includes negative flux fixup. The response matrix (RM) method shows increasing advantage over source iteration (SI) method as the time steps are increased and with increased optical thickness of the slab. For an 80 cm slab calculation under steady state conditions the computing time ratio is (SI/RM) = 3.2 for characteristic differencing.

As in the grey case a companion code was written using a standard source iteration technique in which the space-angle grid is swept for all frequency groups between each update of the temperature distribution. Identical discretizaton techniques are used in both codes to insure validity of the comparisons. Steady state solutions (τ = 0) are tabulated in Table 3 for different slab thicknesses and numbers of mesh points using the step characteristic versions of the codes. The response matrix method is seen to provide consistently superior results.

For the transient calculations shown in Fig. 1, the times are comparable: 8.58 CPU(sec) for the response matrix and 8.92 CPU(sec) for the reference solution. This is thought to be due to the small time step (large τ) which requires no more than few iterations per time step with either of the methods. When diamond differencing (with fixup) is applied, however, the response matrix method requires less than 8 CPU(sec) while the reference method increases to more than 20 CPU(sec); with diamond differencing the reference method requires as many as seven times as many iterations per time step as the response matrix method, even with the small time step.

IV. DISCUSSION

We have demonstrated the use of response matrix methods for an important class of radiative transfer problems in which the radiation and material energy densities are not generally in equilibrium. Response matrix solutions are compared with reference solutions found in the literature and the agreement is excellent. Careful comparison with companion codes for which

the standard source iteration method is employed indicates that for long time steps and for optically thick mesh cells, the method performs very well. For many applications, these are just the problems most frequently encountered.[5]

To fully exploit the method and to assure that the results here apply to more general cases further research is required. Since diffusion synthetic acceleration has been applied to some of the other approaches considered here, an effective acceleration approach for response matrix iterations should be developed, applied and tested. Additionally, much more experience and analyses are needed to test convergence of the response matrix algorithm for wider classes of problems. Finally, the method must be applied to more complicated geometries. The results obtained from simple problems such as those described above encourage further development of the method.

ACKNOWLEDGEMENTS

The authors acknowledge numerous fruitful discussions with Bradley A. Clark of Los Alamos National Laboratory.

REFERENCES

1. S. Lindahl and Z. Weiss, "The Response Matrix Method," Adv. Nucl. Sci. Tech. 13, 72 (1981).

2. R. J. Pryor, "Recent Developments in the Response Matrix Method," in Advanced Reactors: Physics Design in Economics, J. M. Kallfelz and R A. Karam (eds.), Pergamon Press, New York, 1975.

3. G. C. Pomraning, The Equations of Radiation Hydrodynamics, Pergamon Press, New York, 1973.

4. J. A. Fleck, Jr. and J. D. Cummings, Jour. of Comp. Phys. 8, 313-342 (1971).

5. R. E. Alcouffe, B. A. Clark, and E. W. Larsen, "Diffusion Synthetic Acceleration of Transport Iterations, with Application to a Radiation Hydrodynamics Problem," in Multiple Time Scales, J. V. Brackbill and B. I. Cohen (eds.), Academic Press, Orlando, 1985.

6. E. E. Lewis and W. F. Miller, Jr., Computational Methods of Neutron Transport, Wiley Interscience, New York, 1984.

7. Edward W. Larsen and Warren F. Miller, Jr., Nucl. Sci. Eng. 73, 76-83 (1980).

Table 1

Response Matrix Coefficients for Slab Geometry

$$R_m = e^{-\sigma\Delta/|\mu_m|} - \frac{\tau}{\sigma}|\mu_m|\,(1 - e^{-\sigma\Delta/|\mu_m|})^2$$

$$H_m = \left\{ 1 - \frac{\Delta\tau - \frac{|\mu_m|}{\sigma}\tau(1-e^{-\sigma\Delta/|\mu_m|})}{\Delta(\sigma+\tau) - \frac{|\mu_m|}{\sigma}\tau(1-e^{-\sigma\Delta/|\mu_m|})} \right\} \frac{\tau}{\sigma}(1-e^{-\sigma\Delta/|\mu_m|})$$

$$K_m = \left\{ 1 - \frac{[\sigma\Delta - |\mu_m|(1-e^{-\sigma\Delta/|\mu_m|})]\frac{\tau}{\sigma}}{\Delta(\sigma+\tau) - \frac{|\mu_m|}{\sigma}\tau(1-e^{-\sigma\Delta/|\mu_m|})} \right\}(1-e^{-\sigma\Delta/|\mu_m|})$$

$$\tilde{R}_m = \frac{|\mu_m|(1-e^{-\sigma\Delta/|\mu_m|})}{\Delta(\sigma+\tau) - \frac{|\mu_m|\tau}{\sigma}(1-e^{-\sigma\Delta/|\mu_m|})}$$

$$\tilde{H}_m = \frac{[\Delta - \frac{|\mu_m|}{\sigma}(1-e^{-\sigma\Delta/|\mu_m|})]\,\tau}{\Delta(\sigma+\tau) - \frac{|\mu_m|\tau}{\sigma}(1-e^{-\sigma\Delta/|\mu_m|})}$$

$$\tilde{K}_m = \frac{[\Delta - \frac{|\mu_m|}{\sigma}(1-e^{-\sigma\Delta/|\mu_m|})]\,\tau}{\Delta(\sigma+\tau) - \frac{|\mu_m|\tau}{\sigma}(1-e^{-\sigma\Delta/|\mu_m|})}$$

Table 2

CPU(sec) Slab Geometry Grey Steady State Problem

	Thickness = 16 mfp				Thickness = 16 $\sigma\Delta x$			
	Method I & II		Method III		Method I&II		Method III	
$\sigma\Delta x$	CPU(sec)	it*	Cpu(sec)	it*	CPU(sec)	it*	CPU(sec)	it*
0.25	.970	704	.502	167	.042	93	.027	24
0.50	.470	680	.201	132	.084	235	.037	47
1.0	.216	609	.066	86	.210	609	.067	86
2.0	.088	472	.017	43	.490	1399	.097	125
4.0	.034	335	.005	19	.950	2723	.109	142
8.0	.023	239	---	10	1.700	4819	.111	144

*iterations

Table 3

CPU (sec) Grey Transient Problem

Thickness = 16 mfp; $\sigma\Delta x = 0.5$

c(T)	τ	Method I	Method II	Method III
aT^3	.5	2.91	2.24	2.65
aT^3	.05	1.278	0.946	0.588
const.	.05	1.991	---	0.848

Table 4

Multifrequency Steady State Problem

	Δx = T/20				Δx = 1 cm			
T+	RM		Reference		RM		Reference	
	CPU(sec)	it*	CPU(sec)	it*	CPU(sec)	it*	CPU(sec)	it*
20	1.55	63	3.63	178	1.55	63	3.63	178
40	2.04	83	5.00	243	7.43	153	17.62	434
80	2.64	108	6.60	324	38.80	401	--	--

+ Thickness (cm)

* iterations

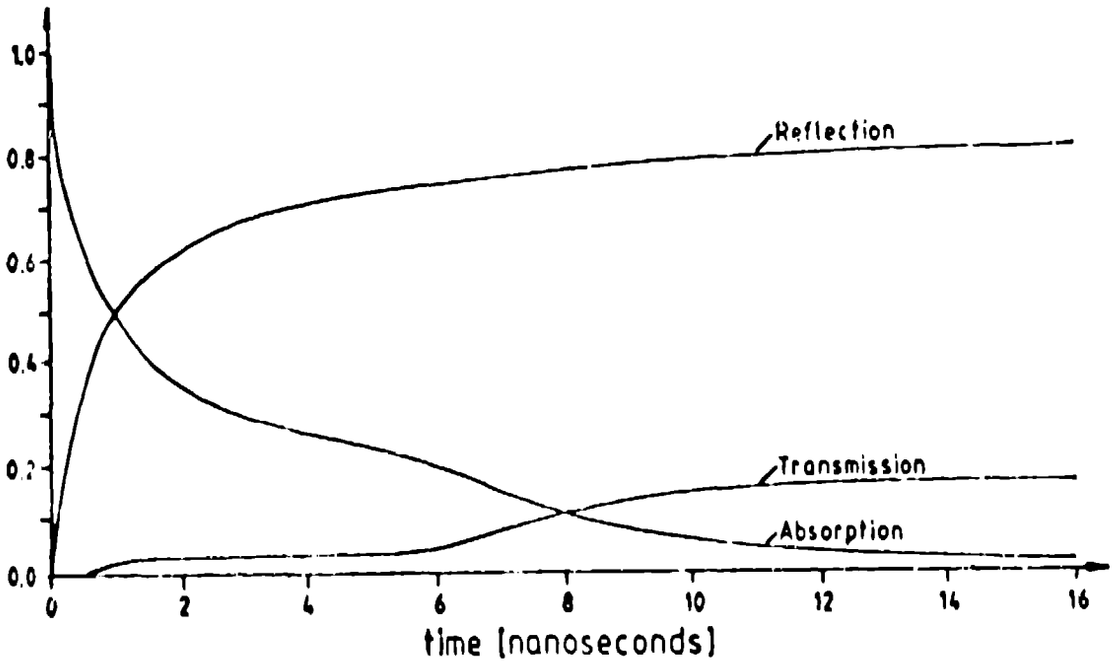

Fig. 1. Fractional Energy Deposition